Geochemistry and mineralogy of Western Australian salt lake sediments: Implications for Meridiani Planum on Mars

Ruecker, A.[1,2], Schröder, C.[3], Byrne, J. [1], Weigold, P. [1], Behrens, S.[1,4], & Kappler, A.[1]*

[1]Geomicrobiology, Center for Applied Geosciences, University of Tuebingen, Germany

[2]Now: Baruch Institute of Coastal Ecology and Forest Science, Clemson University, USA

[3]Biological and Environmental Sciences, School of Natural Sciences, University of Stirling, Scotland, UK

[4]Now: Department of Civil, Environmental, and Geo-engineering, College of Science and Engineering, University of Minnesota, USA

*corresponding author:

Andreas Kappler, Geomicrobiology, Center for Applied Geosciences

University of Tuebingen, Sigwartstraße 10, D-72076 Tübingen, Germany

Phone: +49-7071-2974992, Fax: +49-7071-295059

Email: andreas.kappler@uni-tuebingen.de

For submission to: Astrobiology

Abstract

Hypersaline lakes are characteristic for Western Australia and display a rare combination of geochemical and mineralogical properties which make these lakes potential analogues for past conditions on Mars. In our study we focused on the geochemistry and mineralogy of Lake Orr and Lake Whurr. While both lakes are poor in organic carbon (<1%) the sediments' pH values differ and range from 3.8 to 4.8 in Lake Orr and from 5.4 to 6.3 in Lake Whurr sediments. Lake Whurr sediments were dominated by orange and red sediment zones in which the main Fe minerals were identified as hematite, goethite, and tentatively jarosite and pyrite. Lake Orr was dominated by brownish and blackish sediments where the main Fe minerals were goethite and another paramagnetic Fe(III)-phase that could not be identified. Furthermore, a likely secondary Fe(II)-phase was observed in Lake Orr sediments. The mineralogy of these two salt lakes in the sampling area is strongly influenced by events such as flooding, evaporation and desiccation, processes that explain at least to some extent the observed differences between Lake Orr and Lake Whurr. The iron mineralogy of Lake Whurr sediments and the high salinity make this lake a suitable analogue for Meridiani Planum on Mars and in particular the tentative identification of pyrite in Lake Whurr sediments has implications for the interpretation of the Fe mineralogy of Meridiani Planum sediments.

Key words: Western Australia, salt lakes, jarosite, hematite, pyrite, Mars analogue

Introduction:

The Western Australian wheat belt is characterized by a high number of saline lakes. Although the lakes are located in close proximity to each other, their geochemistry and in particular their pH values are very diverse ranging from strongly acidic with pH <4 to alkaline with pH >8 (Krause *et al.*, 2013). Local events such as flooding, evaporation, desiccation, winds and also groundwater acidity contribute significantly to the geochemical conditions within the salt lakes (Benison *et al.*, 2007). Groundwater acidity in Western Australia is mainly caused by pyrite (FeS_2) oxidation, which was first shown for the Western Australian wheat belt in 1983 (Mann, 1983).

Although the formation of inland saline lakes occurs naturally under arid to semiarid and hot conditions, anthropogenic activities are further contributing to salinization in Western Australia. This anthropogenic salinization is mainly caused by changes in the land use such as the replacement of natural vegetation by agricultural plants which demand irrigation, and thus further increase soil salinity by evapoconcentration (Timms, 2009). In recent years salt lakes located within the Western Australian wheat belt have been suggested as potential new terrestrial analogues for conditions on ancient Mars (Benison and Bowen, 2006; Mormile *et al.*, 2009; Bowen *et al.*, 2012; .

Evidence is accumulating that habitable conditions prevailed during the Noachian period (4.1-3.7 Ga ago) on early Mars (Morris *et al.*, 2010; Squyres *et al.*, 2012; Grotzinger *et al.*, 2014, 2015). Global change towards more acidic aqueous conditions and increasing aridity set in during the late Noachian and Hesperian periods (Bibring *et al.*, 2006). Finely-laminated, S-rich sedimentary bedrock at Meridiani Planum laid down some time during the later Noachian and early Hesperian may represent this later episode. Despite morphological evidence for water pooling episodically at the surface, which suggests temporarily habitable conditions, there is also evidence of evaporation and desiccation (Squyres *et al.,* 2004). Jarosite ($KFe^{3+}_3(SO_4)_2(OH)_6$) in the Meridiani bedrock provides mineralogical evidence for water but indicates that the water was acidic (Klingelhöfer et al., 2004). Desiccation and low pH pose challenges to life and, in particular, prebiotic reactions thought to have played a role in the origin of life (Knoll et la., 2005). Although there is plenty of evidence for the activity of microorganisms under acidic conditions, these highly specialized organisms evolved from organisms originating from less extreme environments (Tehei and Zaccai, 2005; Amils *et al.*, 2014) . Low water activity is the most significant challenge for potential life on Mars. The water activity that has been derived from the evaporative mineral sequence at Meridiani (Tosca *et al.*, 2008) is below the threshold for any known lifeforms on Earth (Grant, 2004; Tosca *et al.*, 2008).

The best known analogue on Earth for Meridiani Planum is the Tinto River in Southern Spain (Fernandez-Remolar *et al.*, 2004; 2005; 2006). While it provides a good mineralogical analogue, it lacks the low water activity/high salinity that comes with the evaporation of briny waters (Ferris *et al.*, 2004). Western Australian salt lake sediments also share relevant characteristics with Meridiani Planum: Besides high salinity these sediments show various examples of low pH environments, the presence of jarosite, the identification of hematite (α-Fe_2O_3) and comparable diagenetic and sedimentological characteristics (Bowen *et al.*, 2008).

When comparing Mars with Earth analogues, one may focus on the Fe (and S) mineralogy because some of the oldest forms of microbial respiration on Earth include Fe(III) and sulfate reduction (Shen *et al.*, 2001; Vargas *et al.*, 1998) Considering the high abundance of Fe(III) and sulfate on the Martian surface in general and at Meridiani in particular, these metabolic pathways are the more likely among those plausible on Mars (Stoker *et al.*, 2010; Nixon *et al.*, 2013), which also include Fe and S oxidation. Further potential electron donors and acceptors to support Fe and S metabolism such as organic matter (Freissinet *et al.*, 2015) or nitrate (Stern *et al.*, 2015) have since been confirmed on Mars. The presence and activity of Fe-metabolizing microorganisms such as *Acidithiobacillus ferrooxidans* or *Leptospirillum sp.* have been shown for the low-pH environment at the Meridiani Planum analogue Rio Tinto (González-Toril *et al.*, 2003). More recently, it was demonstrated that microbial Fe(II) oxidation as well as Fe(III) reduction takes place under conditions up to the solubility limit of NaCl in salt lakes in Southern Russia (Emmerich *et al.*, 2012). However, these salt lakes have neutral to alkaline pH and whether the envelope of Fe metabolism extends to low pH-high salinity environments remains to be shown.

Therefore we were interested in how closely Western Australian salt lakes share relevant iron geochemical and mineralogical characteristics with ancient Mars. We combined geochemical analysis with mineralogical approaches including X-ray diffraction (XRD) and ^{57}Fe-sensitive Mössbauer spectroscopy. While XRD gives insights into the mineralogy in general, ^{57}Fe-sensitive Mössbauer spectroscopy allows the identification of Fe-bearing minerals and different redox states of the Fe present in the mineral structures. The overall goals of this study were (I) to describe the geochemistry and mineralogy from a moderately and a weakly acidic salt lake in Western Australia (Lake Orr and Lake Whurr, respectively), and (II) to enhance our understanding of the potential habitability of Meridiani Planum and Hersperian Mars through the use of the Australian hypersaline lake sediments as analogue environments.

Material and methods

Field site and sampling procedure

Sediment samples were taken from two different hypersaline lakes (in 2012 from Lake Orr and in 2013 from Lake Whurr) in the Western Australian wheat belt (Fig. 1a) (Ruecker *et al.*, 2014, 2015) Lake Orr (33° 8'1.51"S 119° 9'47.14"E) is an acidic and carbon poor salt lake while Lake Whurr (33° 2' 29.30"S 119° 0' 42.02"E) is less acidic and richer in total organic carbon (TOC) with concentrations almost twice as high (Table 1). Lake Orr showed four distinguishable sediment zones, with a whitish salt crust (0-2 cm), a brownish layer (2-5 cm), a dark blackish layer (5-8 cm) and a grayish sediment zone >8 cm (Fig. 1b). Lake Whurr sediments looked fundamentally different from Lake Orr and were dominated by striking orange and red patches distributed throughout the sediments (Fig. 1c). Six sediment cores (30 cm length, 2.5 cm diameter) ranging from the top layer to the deepest layer were taken from each field site for geochemical analysis. Before pulling the cores from the sediment, the top was closed with a butyl rubber stopper. After extraction from the sediment, the bottom of the tube was also closed with a butyl stopper. Additionally, we took bulk samples from the different distinguishable sediment zones. Samples were immediately cooled, and transported at 8°C to the laboratory where samples were stored for a maximum of two weeks at 8°C until further analysis.

Geochemical sediment analyses

For pH measurements 10 g of field fresh sediment were suspended in 25 mL of a 0.01 M $CaCl_2$ solution with pH measured after 2 hours. Total organic carbon was determined from milled sediment samples that were dried at 60°C until weight stability using an Elementar Vario EL element analyzer. Elemental composition of the dried and milled sediments was analyzed using X-ray fluorescence (XRF). Sequential Fe-extractions were performed as described by Porsch and Kappler (2011) with 0.5 and 6 M HCl to distinguish between bioavailable (poorly crystalline) and more crystalline Fe minerals (Piepenbrock *et al.*, 2011; Amstaetter *et al.*, 2012), and subsequent analysis of dissolved iron species was carried out using the spectrophotometric Ferrozine assay (Stookey, 1970). Lake Whurr samples were additionally digested in 6 M anoxic HCl at 70°C. This leads to a complete dissolution of hematite and goethite whereas pyrite partly remains in the solid phase and can be identified using Mössbauer spectroscopy (Heron *et al.*, 1994).

Mineralogical sediment analysis

Micro X-ray diffraction (µXRD) was used to analyze the dried mineral phases using a Bruker D8 Discover X-ray diffraction instrument (Bruker AXS GmbH, Germany) with a Co Kα X-ray tube (λ= 0.179 nm), operating at 30 kV (Berthold *et al.*, 2009). ICDD (International Centre for Diffraction Data) database was used for mineral identification.

Samples for Mössbauer spectroscopy were prepared by loading sediment material (150 mg per sample for Lake Whurr and 136.8 mg per sample for Lake Orr) as dry powder into plexiglas holders (area 1 cm^2). In order to ensure a homogeneous sample with ideal thickness, each sample was mixed and ground using a pestle and mortar. The samples were transferred to the Mössbauer spectrometer and inserted into a closed-cycle exchange gas cryostat (Janis cryogenics). Spectra were collected at 295, 77 and 5 K using a constant acceleration drive system (WissEL) in transmission mode with a ^{57}Co/Rh source and calibrated against a 7 µm thick α-^{57}Fe foil measured at room temperature. Spectra were analyzed with Recoil (University of Ottawa) using the Voigt Based Fitting (VBF) routine (Rancourt and Ping, 1991). The HWHM was fixed to 0.13 mm/s, as determined from the minimum line width of the calibration foil, measured at 295 K.

Results

Geochemical sediment characteristics

The pH values in Lake Orr sediments (sampled in 2012) increased with increasing sediment depth from 3.8 in the salt crust (0-2 cm) to 4.8 in the sediment zone >8 cm. The sediments of Lake Whurr (sampled in 2013) are less acidic and pH increased with increasing sediment depth from 5.5 to 6.3. Total organic carbon (TOC) showed the same spatial pattern and increased with increasing sediment depth from the top sediment zone to the deeper zones and was slightly higher in Lake Whurr sediments (Table 1). Concentrations of leachable organic carbon increased with increasing sediment depth in Lake Orr and ranged from 1.7±0.1 mg L^{-1} to 9.6±0.2 mg L^{-1} >8cm. In Lake Whurr sediments concentrations of leachable organic carbon did not exceed 6.7 mg L^{-1} (red layer) and reached only 2.9 mg L^{-1} in the orange layer.

Fe extractions in Lake Orr sediments using 0.5 M HCl (for the extraction of “poorly crystalline” Fe minerals) showed highest concentrations for total Fe (Fe(tot)) in the depth zone from 5-8 cm (57.3±4.3 µg g^{-1}). The amount of ferrous iron (Fe(II)) of the total iron ranged from 75% in the top 2 cm of the sediments to 66% in the zone from 5-8 cm, and in the zone >8 cm no more ferric iron (Fe(III)) could be detected. When using 6 M HCl (for the extraction of “crystalline” minerals) as

extracting agent, the results looked quite different and we found that the crystalline Fe fraction in Lake Orr sediments was dominated by ferric iron. Lowest Fe(tot) concentrations were found in the top two cm of the profile (10.1±2.9 µg g^{-1}) whereas concentrations in the deeper sediment zones were much higher in the range of 600 µg g^{-1} of Fe(tot). Amounts of Fe(II) of the total iron present in the samples was <3% for the depth zones >2 cm, whereas Fe(II) accounted for 60% of the total iron in the top 2 cm of the sediments (Fig. 2).

For Lake Whurr, total Fe content of 5.2 and 16.2% of the dry weight sediment were quantified for the red and orange sediments, respectively. Sequential Fe-extractions with 1 M and 6 M anoxic HCl demonstrated the presence of Fe(II) in both samples from Lake Whurr. In the “bioavailable”, low crystalline Fe-phase extracted with 1 M anoxic HCl the amount of Fe(II) of the total iron ranged from 10.3% in the orange sample to 9.9% in the red sediments whereas it decreased to 1.3% or 1.6% respectively in the higher crystalline Fe-phase using 6 M anoxic HCl as an extracting agent (Table 2).

Mineralogy of Lake Orr and Lake Whurr sediments – XRD and Mössbauer analyses

Results of the material from the red sediment layer obtained with µXRD suggested the mineral phases were amorphous or nanoparticulate with no clear reflections apart from the background signal of the silicon wafer sample holder (Fig. 3). Material from the orange sediment layer was dominated by halite (NaCl) with minor amounts of goethite (α-FeOOH) and hematite (α-Fe_2O_3).

In order to get more detailed information on the Fe mineralogy and in particular the Fe-redox state in these sediments, we used ^{57}Fe sensitive Mössbauer spectroscopy. ^{57}Fe sensitive Mössbauer spectroscopy is sensitive to iron only. Because it cannot detect mineral phases that do not contain iron such as halite, Mössbauer spectra show also minor Fe-bearing phases otherwise lost in the background. Mössbauer spectroscopy can be used to identify poorly crystalline and amorphous iron minerals.

The major Fe-bearing mineral phases in the orange colored sediment of Lake Whurr are hematite and goethite (Fig. 4), consistent with XRD results. At room temperature, hematite is magnetically ordered (six-line subspectrum) though the magnetic hyperfine field parameter (B_{hf}) (Tab. 3) is smaller than that of pure, well-crystalline hematite. This indicates an amorphous structure and/or impurities such as Al substitutions. Because hematite lines are visible in the XRD pattern, and because the enriched sediment is rich in Al, the latter case is more likely. At lower temperatures, B_{hf} remains below the value expected for pure, well-crystalline hematite. Furthermore, the Morin transition - during which the quadrupole splitting parameter (ΔE_Q) changes from a negative to a

positive value upon lowering the temperature – is suppressed. Both of these observations reinforce the interpretation of an impure hematite. The goethite at room temperature is in the process of magnetic ordering shown by the broad feature in the Mössbauer spectrum. A lowering of the magnetic ordering temperature (Curie temperature T_C of pure, well-crystalline goethite is 400 K; Murad and Cashion, 2004) can be a result of superparamagnetism or again an amorphous structure and/or impurities such as Al substitutions. Superparamagnetism generally occurs at particle sizes below 30 nm. Because goethite is visible in the XRD pattern, we again favor an Al-substituted goethite as explanation.

The Mössbauer spectra reveal two additional two-line subspectra (doublets) that have no equivalent in the XRD pattern. For one of these doublets, the combination of the center shift value (CS) of 0.38 and ΔE_Q of 1.31 at room temperature (Tab. 3) indicates a high spin Fe(III) compound. This phase appears to be paramagnetic as the increase in the ΔE_Q parameter between 77 K and 5 K suggests the onset of magnetic ordering. The Mösbauer parameters at room temperature are consistent with the Fe(III) sulfate hydroxide jarosite. Jarosite usually forms at pH values lower than those determined for Lake Whurr but the dissolution of pyrite can lower the pH locally into the jarosite stability range (McHenry *et al.* 2011).

The room temperature parameters of the other doublet (Tab. 3) would be consistent with both a high spin Fe(III) compound or a low spin Fe(II) compound (e.g. Murad and Cashion 2004; Gütlich and Schröder 2012, and references therein). The ΔE_Q parameter stays constant from room temperature down to 5 K, suggesting a diamagnetic mineral phase. The low spin Fe(II) mineral pyrite is one of the very few Fe minerals known to be diamagnetic. Although the parameters fall at the edge of the range of Mössbauer parameters that have been reported for pyrite (Stevens *et al.* 2002), we therefore tentatively assign this phase to pyrite. There is a line of evidence backing up this assignment. First of all, pyrite is the reason for acidic ground water in Western Australia (Mann, 1983) and it would be consistent with the observation of jarosite. Secondly, there is sufficient S in the sediment (Tab. 1). And thirdly, acid extractions of the sediment with 1 M anoxic HCl and subsequent determination of the Fe(II) with the Ferrozine assay showed that ~10% of Fe(tot) are present as Fe(II) (Tab. 2), which is comparable to the percentage of Fe(tot) (parameter relative population (Pop.) in Tab. 3) in pyrite. This first step extracts the bioavailable, poorly crystalline Fe phases. A second extraction with 6 M HCl for the non-bioavailable, crystalline Fe-phases reveals little Fe(II). However, crystalline pyrite is not soluble in acid. Mössbauer spectra of the residual material after the second extraction step (Fig. 5, Tab. 4) are consistent with pyrite.

Mössbauer spectra of samples stemming from the red sediments from Lake Whurr contain only hematite as major Fe mineral and no goethite (Fig. 4, Tab. 3). There appears to be a range of hematite fractions of different particle sizes and/or crystallinities. Three fractions are represented in the room temperature spectrum: a magnetically ordered component with a well-resolved six-line pattern, a component in the process of magnetic ordering, and a superparamagnetic component. The second component is fully ordered in the 77 K spectrum. The superparamagnetic component is represented by a doublet and persists at 77 K before it becomes magnetically ordered at 5 K, which is indicated by the decrease in the ΔE_Q parameter in the remaining doublet. The hematite in the red sample is therefore less crystalline than the hematite in the orange sample, which is consistent with the XRD observation of only amorphous mineral phases. As in the orange sample, B_{hf} values are lower than those of pure, well-crystalline hematite and the Morin transition is suppressed, which suggests possible Al substitution.

A doublet remains at 5 K with the same parameters as the doublet assigned to pyrite in the orange sample. We therefore again tentatively assign this phase to pyrite, supported by the identification of Fe(II) in the acid extraction results (Tab. 2). The pyrite and superparamagnetic hematite doublets overlap and cannot be resolved in the higher temperature spectra. There is no indication of jarosite in the room temperature and 77 K spectra though we could fit a jarosite doublet into the 5 K spectrum. With 2 % Pop. it is at the detection limit generally quoted for Mössbauer spectroscopy and we therefore conclude that, if jarosite is present in the red sample, it is at or below the detection limit.

The mineralogy of Lake Orr looks different compared to the results from Lake Whurr. Fe minerals of 2 sediment zones (2-5 cm and 5-8 cm depth) were identified using ^{57}Fe-sensitive Mössbauer spectroscopy only (Fig. 6). Figure 6a shows the results for the zone from 2-5 cm for measurements at room temperature, 77 K and 5 K. When measured at room temperature, the Mössbauer spectrum for a sample from a depth zone from 2-5 cm is dominated by a (super)paramagnetic Fe(III) phase which accounts for 97.4% of the total spectral area. Additionally, there is an Fe(II) phase which accounts for 2.6%. As temperature is decreased, magnetic ordering increases and a sextet becomes visible at 77 K which accounts for 13.6% of the total spectral area. At 5 K the magnetically ordered Fe(III) phase is identified as goethite and accounts for 27.5% while the (super)paramagnetic Fe(III) phase accounts for 66.9% and the Fe(II) phase for 5.6% of the total spectral area. The fact that the identified goethite becomes visible only under low temperatures suggests a very small particle size, resulting in a very low blocking temperature. The remaining doublet may still be superparamagnetic goethite with very small particle sizes (van der Zeee *et al.*

2003). Another explanation might be the incorporation of additional elements such as aluminum in the crystal structure (Murad and Schwertmann, 1983).

The sediment from 5-8 cm shows similar characteristics as the one from 2-5 cm (Fig. 6b). The room temperature spectrum is dominated by a doublet which is characteristic of a superparamagnetic or poorly crystalline Fe(III) mineral (81.9% of the total spectral area). Additionally, a poorly defined sextet was required to fit the data. Surprisingly this sextet was not apparent when measured at 77 K. However, this is probably caused by the poor signal to noise ratio for this particular measurement and consequently the sextet could not be distinguished from the background. At 5 K the sextet accounting for 21.5% of the total spectral area was identified as nano-goethite. 76.5% of the total spectral area corresponded to a poorly crystalline Fe(III) phase. The Fe(II) phase which was also identified in the sediment zone from 2-5 cm was detected at all temperatures (2.0-5.3% of the spectral area) in the sediment depth zone from 5-8 cm as well. The presence of Fe(II) in Lake Orr samples was also confirmed by sequential Fe-extractions (Fig. 2). Mössbauer parameters for the samples from 2-5 cm and 5-8 cm are presented in Table 5.

Discussion

Geochemistry of Lake Orr and Lake Whurr sediments depending on rainfall events

Geochemical parameters revealed fundamental differences between Lake Orr and Lake Whurr. Not only is Lake Orr more acidic than Lake Whurr, but also the concentrations of total Fe in % were considerably lower in Lake Orr compared to Lake Whurr. When comparing the amounts of Fe(II) of the total Fe, it becomes evident that conditions were more reduced in Lake Orr in 2012 compared to Lake Whurr in 2013. While we did not detect any ferric Fe at all in Lake Orr sediments >8 cm depth, the amounts of Fe(II) of the total Fe in the orange layer of Lake Whurr did not exceed 10.3% in the low crystalline Fe-phase. The occurrence of reducing conditions in Lake Orr sediments is additionally supported by the dark black color in the sediment zone >8 cm, probably indicating the presence of sulfide and thus microbial sulfate reduction (Mesbah *et al.*, 2007; Porter *et al.*, 2007). One of the reasons for the predominance of reducing conditions in Lake Orr sediments but not in Lake Whurr sediments (despite the higher TOC in Lake Whurr sediments) is probably the thick (several cm) salt crust present at Lake Orr in 2012 limiting oxygen penetration and allowing the establishment of reducing conditions. In contrast, the sediment samples taken at Lake Whurr in 2013 had a very different appearance and no salt crust was present. Instead, the top cm of the sediments had a sand-like coarse structure probably allowing better oxygen penetration than the salt crust at Lake Orr. This difference in the two sediments was probably caused by the very different weather conditions during sampling in the years 2012 and 2013.

During sampling in 2012 the weather conditions were dry and before sampling it had not rained for at least 12 weeks and thus the lakebed of Lake Orr was completely desiccated with a 3-4 cm thick salt crust covering the whole lake surface. In contrast, there was heavy rainfall in the weeks prior to the 2013 sampling campaign at Lake Whurr. Therefore, the lakebed was filled with water with an average water depth of 15 cm (Fig. 1d, e). This led to dissolution of most of the salt crust and consequently to completely different geochemical conditions in the sediments. The relevance of changing weather conditions on sedimentary geochemical conditions within Western Australian salt lakes has been shown previously (Benison *et al.*, 2007). Rainfall in the days right before sampling of Lake Whurr in 2013 led to the dissolution of the evaporate crystals (mainly halite) and due to the inflow of fresh water to a decrease in salinity and an increase in pH. Due to dry conditions in the following days, the lake was in the so called "evapoconcentration state" during sampling of Lake Whurr in 2013. This leads to the precipitation of halite and partly also gypsum crystals from the water, a decrease in the pH, while salinity increases again as water evaporates (Benison *et al.*, 2007). Additionally hematite and jarosite precipitation has been observed to occur during the evapoconcentration stage (Benison *et al.*, 2007). In contrast to that, during the sampling campaign in the Australian autumn 2012, Lake Orr was probably in the so-called desiccation stage. In this stage precipitation of evaporate crystals continues and leads to cm-thick halite or gypsum crusts as also observed at Lake Orr in 2012. Due to the thickening of the salt crust oxygen penetration is limited resulting in oxygen limitation and the occurrence of reducing conditions. This was confirmed by the quantification of reduced iron (Fe(II)) and a black sediment color of the Lake Orr sediments suggesting microbial sulfate reduction (Foti *et al.*, 2007; Sorokin *et al.*, 2012).

Mineralogy of Lake Orr and Lake Whurr sediments

^{57}Fe-Mössbauer spectroscopy analysis of Lake Orr as well as Lake Whurr sediments showed that the Fe minerals in both spectra were dominated by Fe(III) phases and that Fe(II) plays a minor role only. Goethite was identified in Lake Orr sediments from both layers analyzed (2-5 cm and 5-8 cm) and the fact that the Mössbauer spectra of these samples are dominated by a doublet at room temperature suggests that the Fe minerals present have a very small particle size. The presence of nanoparticular goethite is in line with results from boreal lake sediments and marine sediments where nanogoethite (2-12 nm particle size) was also identified as the dominant reactive oxyhydroxide phase (van der Zee *et al.*, 2003). The goethite could be formed under such conditions either by abiotic Fe(II) oxidation, by Fe(II)-oxidizing bacteria or even by transformation of ferrihydrite-like ferric iron hydroxides (Schwertmann and Cornell, 1996; Posth *et al.*, 2014).

In Lake Whurr sediments, goethite is present at larger particle sizes together with hematite in the orange sample. The red sample contains hematite but no goethite. The precipitation of hematite is characteristic for acid saline lakes in southern Western Australia and can occur either directly from oxidation of Fe(II) stemming from groundwater and lake water or during dissolution and reprecipitation of other mineral phases (Benison and Bowen, 2006) The source of the iron that composes the hematite and goethite is probably the highly weathered underlying bedrock (Anand and Paine, 2002; Bowen *et al.*, 2008). Additionally, the breakdown of the Fe-bearing sulfate jarosite has been suggested as a possible Fe source in Western Australian salt lakes (Bowen *et al.*, 2008).

Jarosite formation has mainly been described for acidic environments at pH values ranging from <2 to an upper pH limit of about 5.6 (Küsel *et al.*, 1999; Fernández-Remolar *et al.*, 2005; Knoll *et al.*, 2005; Bowen and Benison, 2009). It has been suggested that pyrite oxidation which results in the formation of sulfuric acid (H_2SO_4), might locally lower the pH into the stability field of jarosite (McHenry *et al.*, 2011). This is also conceivable for Lake Whurr where the overall pH was only mildly acidic. In particular as the orange minerals containing the jarosite were not distributed evenly throughout the sediments but appeared in localized, small lenses and patches of minerals (Fig. 1), reactions at the small scale leading to locally acidic conditions favoring jarosite precipitation might have occurred. Such localized jarosite precipitates have been identified before in acidic microenvironments in highly carbonate-buffered sediments of a polar desert (Leveille, 2007) or against an alkaline backdrop in the African rift valley (McHenry *et al.* 2011).

A direct precipitation of the Fe-minerals hematite and also goethite at our two field sites is possible (Benison and Bowen, 2006). In particular during evaporation and desiccation salts such as halide, but also hematite and goethite are known to precipitate from lake waters and can form small mm- and cm-sized patches of e.g. hematite as seen in Fig.1b (Benison *et al.*, 2007). Additionally, abiotic and microbially initiated dissolution and reprecipitation of Fe-minerals is likely to happen at our field sites in Western Australia (Schwertmann and Cornell, 1996; Posth *et al.*, 2014), probably stimulated by the dry- and wet cycles occurring during flooding, evaporation and desiccation. In particular during flooding reducing conditions could lead to microbial Fe(III) reduction and to the formation of Fe(II). As a consequence, Fe(II)-catalyzed transformation of Fe minerals can occur, also leading to the formation of goethite (Hansel *et al.*, 2003; Hansel *et al.*, 2005).

Lake Whurr as a terrestrial Mars analogue

The minerals identified in Lake Whurr sediments and the sediment geochemistry suggests that Lake Whurr is a suitable terrestrial analogue to study mineral (trans)formation pathways at

Meridiani Planum on Mars, where hematite, and jarosite have been identified (Klingelhöfer *et al.*, 2004). Although salt lakes in the Western Australian wheat belt have already been suggested as terrestrial Mars analogues, most studies have focused on strongly acidic salt lakes with pH values <4 (Benison and Bowen, 2006; Bowen *et al.*, 2008). However, we have identified the presence of hematite, goethite and tentatively jarosite in mildly acidic salt lake sediments from Lake Whurr. Thus also mildly acidic environments might be considered as terrestrial analogues for past conditions at Meridiani Planum on Mars.

Another interesting mineralogical aspect is the tentative identification of pyrite (FeS_2) in Lake Whurr sediments. Although it has been suggested to be characteristic of acidic Western Australian salt lakes (Krause *et al.*, 2013), the Mössbauer parameters identified for the potential pyrite mineral phase from Lake Whurr (Table 3, Table 4) are similar to the parameters of the Fe3D3 mineral phase identified in the S-rich Meridiani Planum sedimentary rocks on Mars (Klingelhöfer *et al.* 2004; Morris *et al.* 2006). This Fe3D3 mineral phase has been suggested to be a nanophase Fe(III) (oxyhydr)oxide, the sulfate mineral schwertmannite, or possibly a phylloslicate (Klingelhöfer *et al.* 2004; Morris *et al.* 2006) but pyrite has not been considered as a possibility. There is a slight negative correlation between Fe3D3 and S in Meridiani sedimentary rocks (Clark *et al.*, 2005), and therefore pyrite may only be a fraction contributing to the Fe3D3 doublet. If pyrite were present at Meridiani, it would increase Fe(II)/Fe(tot) ratios, and the conditions during formation and diagenesis of the sedimentary at Meridiani might have been less oxidizing than thought.

Apart from the mineralogy, the microbial community of Western Australian salt lakes has been investigated recently as well and the studies demonstrated that there is a diverse microbial community present dominated by species expected in saline environments such as *Salinibacter ruber* or *Salinisphaera shabanensis* (Benison *et al.*, 2008; Mormile *et al.*, 2009; Benison and Bowen, 2013; Weigold *et al.*, 2015). Very recently a metagenomic approach was used to describe not only the microbial community of a salt lake in Western Australia, but also to identify its metabolic potential. This study demonstrated that most of the identified genes were associated to sulfur metabolism (Johnson *et al.*, 2015). However, these studies did not investigate the presence or even activity of Fe-metabolizing microorganisms and their contribution to the mineral formation and transformation in salt lake sediments. Generally, knowledge on microbial Fe-redox processes under elevated salinities is rather limited and only very few isolated bacterial strains are known (Pollock *et al.*, 2007; Oren, 2011). One study on sediments in a Russian salt lake showed the presence and activity of Fe(II)-oxidizing and Fe(III)-reducing microorganisms up to the solubility limit of NaCl (Emmerich *et al.*, 2012). These Russian salt lakes are also of interest since among the minerals identified in their sediments there was akaganéite (FeO(OH)Cl. Akaganéite is an iron

oxyhydroxide mineral characterized by the incorporation of Cl^- into the layered mineral structure that is known to occur in saline environments (Schwertmann and Cornell, 2007; Bibi *et al.*, 2011). Akaganéite has been shown to form by both abiotic and biotic processes (Holm *et al*., 1983; 1993, Xiong *et al.*, 2008 Chan *et al.*, 2009;) and has also been suggested as a precursor for the hematite minerals on Mars (Glotch and Kraft, 2008) and its presence on Mars has recently been verified using orbital imaging spectroscopy (Carter *et al.*, 2015). However, akaganéite was not detected in the Australian salt lake sediments. One reason for this might have been the differences in the salinity between Lake Kasin and Lake Whurr. With salinities above the solubility limit of NaCl, Lake Kasin has been more saline than Lake Whurr. This lower salinity of Lake Whurr was mainly caused by the heavy rainfall prior to sampling in 2013 which had a diluting effect on the salinity in Lake Whurr. It can be assumed that the lower salinities of Lake Whurr promoted the formation of minerals such as hematite or jarosite over the formation of the Cl-containing akaganéite.

The highly acidic Rio Tinto in Spain, another terrestrial analogue for Meridiani Planum, sustains a microbially driven Fe-redox cycle (Amils *et al.*, 2014). The presence of Fe(II)-oxidizers such as *Leptospirillum ferrooxidans*, but also Fe(III)-reducing microorganisms, e.g. *Acidiphilium spec.* has been shown (González-Toril *et al.*, 2003). Additionally, *Acidithiobacillus ferrooxidans* was identified, a bacterium that can oxidize Fe(II) and reduce Fe(III) (Ohmura *et al.*, 2002; Malki *et al.*, 2006). Fe-based metabolism has thus been demonstrated in highly acidic (Rio Tinto) and hypersaline environments (Russian salt lakes). The presence and activity of Fe-metabolizing microorganisms is also likely to occur in the saline and mildly acidic Lake Whurr sediments. Whether a comparable microbial metabolism would also be possibly under the acidic conditions and low water activity derived for Meridiani Planum remains to be demonstrated.

Acknowledgements

The authors would like to thank Ellen Struve for TIC/TOC and leachable organic carbon measurements and Heiner Taubald for XRF measurements. Furthermore we would like to acknowledge Christoph Berthold for assistance during µXRD measurements and Heinfried Schöler, Cornelius Zetzsch, Andreas Held, Johannes Ofner, Torsten Krause and Katharina Kamili for their help during sampling in Australia. This work was funded by the DFG research unit 763 Natural Halogenation processes in the environment-soil and atmosphere.

Author Disclosure Statement

No competing financial interests exist.

References

Amils, R., Fernández-Remolar, D., IPBSL Team. (2014) Río Tinto: A Geochemical and Mineralogical Terrestrial Analogue of Mars. *Life* 4:511–534.

Amstaetter, K., Borch, T., Kappler, A. (2012) Influence of humic acid imposed changes of ferrihydrite aggregation on microbial Fe(III) reduction. *Geochim. Cosmochim. Acta 85*:326–341.

Anand, R.R., Paine, M. (2002) Regolith geology of the Yilgarn Craton, Western Australia: implications for exploration. *Aust. J. Earth Sci.* 49:3–162.

Benison, K.C., Bowen, B.B. (2013) Extreme sulfur-cycling in acid brine lake environments of Western Australia. *Chem. Geol.* 351:154–167.

Benison, K.C., Bowen, B.B. (2006) Acid saline lake systems give clues about past environments and the search for life on Mars. *Icarus* 183:225–229.

Benison, K.C., Bowen, B.B., Oboh-Ikuenobe, F.E., Jagniecki, E.A., LaClair, D.A., Story, S.L., Mormile, M.R., Hong, B.Y. (2007) Sedimentology of acid saline lakes in southern Western Australia: newly described processes and products of an extreme environment. *J. Sediment. Res.* 77:366–388.

Benison, K.C., Jagniecki, E.A., Edwards, T.B., Mormile, M.R., Storrie-Lombardi, M.C. (2008) "Hairy blobs:" microbial suspects preserved in modern and ancient extremely acid lake evaporites. *Astrobiology* 8:807–821.

Berthold, C., Bjeoumikhov, A., Brügemann, L. (2009) Fast XRD_2 Microdiffraction with focusing X-ray microlenses. *Part.& Part. Syst. Charact*. 26:107–111.

Bibi, I., Singh, B., Silvester, E. (2011) Akaganéite (β-FeOOH) precipitation in inland acid sulfate soils of south-western New South Wales (NSW), Australia. *Geochim. Cosmochim. Acta* 75: 6429–6438.

Bibring, J.-P., Langevin, Y., Mustard, J.F., Poulet, F., Arvidson, R., Gendrin, A., Gondet, B., Mangold, N., Pinet, P., Forget, F. (2006) Global mineralogical and aqueous Mars history derived from OMEGA/Mars Express data. *Science* 80, 312:400–404.

Bowen, B.B., Benison, K.C. (2009) Geochemical characteristics of naturally acid and alkaline saline lakes in southern Western Australia. *Appl. Geochemistry* 24:268–284.

Bowen, B.B., Benison, K.C., Oboh-Ikuenobe, F.E., Story, S., Mormile, M.R. (2008) Active hematite concretion formation in modern acid saline lake sediments, Lake Brown, Western Australia. *Earth Planet. Sci. Lett.* 268:52–63.

Bowen, B.B., Benison, K.C., Story, S. (2012) Early diagenesis by modern acid brines in Western Australia and implications for the history of sedimentary modification on Mars. *Soc. Sediment. Geol. Spec. Publ. Mars Sedimentol. SEPM Spec. Publ.* 102:229–252.

Carter, J., Viviano-Beck, C., Loizeau, D., Bishop, J., Le Deit, L. (2015) Orbital detection and implications of akaganéite on Mars. *Icarus* 253:296–310.

Chan, C.S., Fakra, S.C., Edwards, D.C., Emerson, D., Banfield, J.F. (2009) Iron oxyhydroxide mineralization on microbial extracellular polysaccharides. *Geochim. Cosmochim. Acta 73*:3807–3818.

Clark, B.C., Morris, R. V, McLennan, S.M., Gellert, R., Jolliff, B., Knoll, A.H., Squyres, S.W., Lowenstein, T.K., Ming, D.W., Tosca, N.J. (2005) Chemistry and mineralogy of outcrops at Meridiani Planum. *Earth Planet. Sci. Lett.* 240:73–94.

Emmerich, M., Bhansali, A., Lösekann-Behrens, T., Schröder, C., Behrens, S. (2012) Abundance, Distribution, and Activity of Fe(II)-Oxidizing and Fe(III)-Reducing Microorganisms in Hypersaline Sediments of Lake Kasin, Southern Russia. *Appl. Environ. Microbiol*. 78:4386–4399.

Fernández-Remolar, D., Gómez-Elvira, J., Gómez, F., Sebastian, E., Martíin, J., Manfredi, J. A., Torres, J., González Kesler, C., Amils, R. (2004) The Tinto River, an extreme acidic environment under control of iron, as an analog of the Terra Meridiani hematite site of Mars. *Planet. Space Sci.* 52:239–248.

Fernández-Remolar, D.C., Morris, R. V, Gruener, J.E., Amils, R., Knoll, A.H. (2005) The Río Tinto Basin, Spain: mineralogy, sedimentary geobiology, and implications for interpretation of outcrop rocks at Meridiani Planum, Mars. *Earth Planet. Sci. Lett.* 240:149–167.

Fernández-Remolar, D.C., Prieto-Ballesteros, O., Chemtob, S.M., Morris, R. V, Ming, D., Knoll, A.H., Hutchison, L., Mustard, J.F., Amils, R., Arvidson, R.E. (2006) Geochemical processes driving the Rio Tinto acidic sedimentation: insights into sedimentary sequences on early Mars, in: *37th Annual Lunar and Planetary Science Conference*. p. 1809.

Ferris, F.G., Hallbeck, L., Kennedy, C.B., Pedersen, K. (2004) Geochemistry of acidic Rio Tinto headwaters and role of bacteria in solid phase metal partitioning. *Chem. Geol.* 212:291–300.

Foti, M., Sorokin, D.Y., Lomans, B., Mussman, M., Zacharova, E.E., Pimenov, N. V, Kuenen, J.G., Muyzer, G. (2007) Diversity, activity, and abundance of sulfate-reducing bacteria in saline and hypersaline soda lakes. *Appl. Environ. Microbiol.* 73:2093–100.

Freissinet, C., Glavin, D.P., Mahaffy, P.R., Miller, K.E., Eigenbrode, J.L., Summons, R.E., Brunner, A.E., Buch, A., Szopa, C., Archer, P.D. (2015) Organic molecules in the Sheepbed Mudstone, Gale Crater, Mars. *J. Geophys. Res. Planets* 120:495–514.

Glotch, T.D., Kraft, M.D. (2008) Thermal transformations of akaganite and lepidocrocite to hematite: Assessment of possible precursors to Martian crystalline hematite. *Phys. Chem. Miner.* 35:569–581.

González-Toril, E., Llobet-Brossa, E., Casamayor, E.O., Amann, R., Amils, R. (2003) Microbial ecology of an extreme acidic environment, the Tinto River. *Appl. Environ. Microbiol.* 69:4853–4865.

Grant, W.D. (2004) Life at low water activity. *Philos. Trans. R. Soc. London B Biol. Sci.* 359:1249–1267.

Grotzinger, J.P., Gupta, S., Malin, M.C., Rubin, D.M., Schieber, J., Siebach, K., Sumner, D.Y., Stack, K.M., Vasavada, A.R., Arvidson, R.E., Calef, F., Edgar, L., Fischer, W.F., Grant, J.A., Griffes, J., Kah, L.C., Lamb, M.P., Lewis, K.W., Mangold, N., Minitti, M.E., Palucis, M., Rice, M., Williams, R.M.E., Yingst, R.A., Blake, D., Blaney, D., Conrad, P., Crisp, J., Dietrich, W.E., Dromart, G., Edgett, K.S., Ewing, R.C., Gellert, R., Hurowitz, J.A., Kocurek, G., Mahaffy, P., McBride, M.J., McLennan, S.M., Mischna, M., Ming, D., Milliken, R., Newsom, H., Oehler, D., Parker, T.J., Vaniman, D., Wiens, R.C., Wilson, S.A. (2015) Deposition, exhumation, and paleoclimate of an ancient lake deposit, Gale crater, Mars. *Science* 350:6257

Grotzinger, J.P., Sumner, D.Y., Kah, L.C., Stack, K., Gupta, S., Edgar, L., Rubin, D., Lewis, K., Schieber, J., Mangold, N. (2014) A habitable fluvio-lacustrine environment at Yellowknife Bay, Gale Crater, Mars. *Science* 343:1242777.

Gütlich P., Schröder, C. (2012) Mössbauer Spectroscopy. In: Schäfer R, Schmidt PC (ed.). Methods in Physical Chemistry, Weinheim, Germany: Wiley-VCH, pp. 351-389

Hansel, C.M., Benner, S.G., Neiss, J., Dohnalkova, A., Kukkadapu, R.K., Fendorf, S. (2003) Secondary mineralization pathways induced by dissimilatory iron reduction of ferrihydrite under advective flow. *Geochim. Cosmochim. Acta* 67:2977–2992.

Hansel, C.M., Benner, S.G., Fendorf, S. (2005) Competing Fe (II)-induced mineralization pathways of ferrihydrite. *Environ. Sci. Technol.* 39:7147–7153.

Heron, G., Crouzet, C., Bourg, A.C.M., Christensen, T.H. (1994) Speciation of Fe(II) and Fe(III) in Contaminated Aquifer Sediments Using Chemical Extraction Techniques. *Environ. Sci. Technol.* 28:1698–1705.

Holm, N.G., Dowler, M.J., Wadsten, T., Arrhenius, G. (1983) β-FeOOH· Cl n (akaganéite) and Fe 1-x O (wüstite) in hot brine from the Atlantis II Deep (Red Sea) and the uptake of amino acids by synthetic β-FeOOH· Cl n. *Geochim. Cosmochim. Acta 47*:1465–1470.

Holm, N.G., Ertem, G., Ferris, J.P. (1993) The binding and reactions of nucleotides and polynucleotides on iron oxide hydroxide polymorphs. *Orig. Life Evol. Biosph. 23*, 195–215.

Johnson, S.S., Chevrette, M.G., Ehlmann, B.L., Benison, K.C. (2015) Insights from the metagenome of an acid salt lake: The role of biology in an extreme depositional environment. *PLoS One* 10(4):e0122869.

Klingelhöfer, G., Morris, R. V, Bernhardt, B., Schröder, C., Rodionov, D.S., de Souza, P.A., Yen, A., Gellert, R., Evlanov, E.N., Zubkov, B., Foh, J., Bonnes, U., Kankeleit, E., Gütlich, P., Ming, D.W., Renz, F., Wdowiak, T., Squyres, S.W., Arvidson, R.E. (2004) Jarosite and hematite at Meridiani Planum from Opportunity's mössbauer spectrometer. *Science* 306:1740–5.

539 Knoll, A.H., Carr, M., Clark, B., Des Marais, D.J., Farmer, J.D., Fischer, W.W., Grotzinger, J.P.,
540 McLennan, S.M., Malin, M., Schröder, C. (2005) An astrobiological perspective on Meridiani
541 Planum. *Earth Planet. Sci. Lett.* 240:179–189.

542 Krause, T., Tubbesing, C., Benzing, K., Schöler, H.F. (2013) Model reactions and natural
543 occurrence of furans from hypersaline environments. *Biogeosciences Discuss.* 10:17439–
544 17468.

545 Küsel, K., Dorsch, T., Acker, G. (1999) Microbial reduction of Fe(III) in acidic sediments :
546 Isolation of *Acidiphilium cryptum* JF-5 capable of coupling the reduction of Fe(III) to the
547 oxidation of glucose. *Appl. Environ. Micrbiol.* 1999, 65(8):3633-3640.

548 Leveille, R.J. (2007) Formation of jarosite and Mars-like minerals in a polar desert: implications
549 for Mars aqueous geochemistry, in: *2007 GSA Denver Annual Meeting*.

550 Malki, M., González-Toril, E., Sanz, J.L., Gómez, F., Rodríguez, N., Amils, R. (2006) Importance
551 of the iron cycle in biohydrometallurgy. *Hydrometallurgy* 83:223–228.

552 Mann, A.W. (1983) Hydrogeochemistry and weathering on the Yilgarn Block, Western
553 Australia—ferrolysis and heavy metals in continental brines. *Geochim. Cosmochim. Acta*
554 47:181–190.

555 McHenry, L.J., Chevrier, V., Schörder, C. (2011) Jarosite in a Pleistocene East African saline-
556 alkaline paleolacustrine deposit: Implications for Mars aqueous geochemistry. *J. Geophys.*
557 *Res. E Planets* 116:1-15.

558 Mesbah, N., Abou-El-Ela, S., Wiegel, J. (2007) Novel and unexpected prokaryotic diversity in
559 water and sediments of the alkaline, hypersaline lakes of the Wadi An Natrun, Egypt.
560 *Microb. Ecol.* 54:598–617.

561 Mormile, M.R., Hong, B.-Y., Benison, K.C. (2009) Molecular analysis of the microbial
562 communities of Mars analog lakes in Western Australia. *Astrobiology* 9:919–930.

563 Morris, R. V, Ruff, S.W., Gellert, R., Ming, D.W., Arvidson, R.E., Clark, B.C., Golden, D.C.,
564 Siebach, K., Klingelhöfer, G., Schröder, C. (2010) Identification of carbonate-rich outcrops
565 on Mars by the Spirit rover. *Science* 329:421–424.

566 Morris, R. Van, Klingelhöfer, G., Schröder, C., Rodionov, D.S., Yen, A., Ming, D.W., De Souza,
567 P.A., Wdowiak, T., Fleischer, I., Gellert, R. (2006) Mössbauer mineralogy of rock, soil, and
568 dust at Meridiani Planum, Mars: Opportunity's journey across sulfate-rich outcrop, basaltic
569 sand and dust, and hematite lag deposits. *J. Geophys. Res. Planets* 111.

570 Murad, E., Cashion, J. (2004) Iron Oxides, in: Mössbauer Spectroscopy of Environmental
571 Materials and Their Industrial Utilization. Springer, pp. 159–188.

572 Murad, E., Schwertmann, U. (1983) The influence of aluminium substitution and crystallinity on
573 the Mossbauer spectra of goethite. *Clay Min*. 18:301–312.

574 Nixon, S.L., Cockell, C.S., Cousins, C.R. (2013) Plausible microbial metabolisms on Mars.
575 *Astron. Geophys*. 54:13–16.

576 Ohmura, N., Sasaki, K., Matsumoto, N., Saiki, H. (2002) Anaerobic respiration using Fe^{3+}, S0,
577 and H_2 in the chemolithoautotrophic bacterium *Acidithiobacillus ferrooxidans*. *J. Bacteriol.*
578 184:2081–2087.

579 Oren, A. (2011) Thermodynamic limits to microbial life at high salt concentrations. *Environ.*
580 *Microbiol*. 13:1908–23.

581 Piepenbrock, A., Dippon, U., Porsch, K., Appel, E., Kappler, A. (2011) Dependence of microbial
582 magnetite formation on humic substance and ferrihydrite concentrations. *Geochim.*
583 *Cosmochim. Acta* 75:6844–6858.

584 Pollock, J., Weber, K. a, Lack, J., Achenbach, L. a, Mormile, M.R., Coates, J.D. (2007) Alkaline
585 iron(III) reduction by a novel alkaliphilic, halotolerant, *Bacillus sp*. isolated from salt flat
586 sediments of Soap Lake. *Appl. Microbiol. Biotechnol.* 77:927–934.

587 Porsch, K., Kappler, A. (2011) Fe(II) oxidation by molecular O_2 during HCl extraction. *Environ.*
588 *Chem.* 8:190-197.

589 Porter, D., Roychoudhury, A.N., Cowan, D. (2007) Dissimilatory sulfate reduction in hypersaline
590 coastal pans: Activity across a salinity gradient. *Geochim. Cosmochim. Acta* 71:5102–5116.

591 Posth, N.R., Canfield, D.E., Kappler, A. (2014) Biogenic Fe (III) minerals: from formation to
592 diagenesis and preservation in the rock record. *Earth-Science Rev.* 135:103–121.

593 Rancourt, D.G., Ping, J.Y. (1991) Voigt-based methods for arbitrary-shape static hyperfine
594 parameter distributions in Mössbauer spectroscopy. Nucl. Instruments Methods Phys. Res.
595 Sect. B Beam Interact. with Mater. *Atoms* 58:85–97.

596 Ruecker, A., Weigold, P., Behrens, S., Jochmann, M., Laaks, J., Kappler, A (2014)
597 Predominance of Biotic over Abiotic Formation of Halogenated Hydrocarbons in
598 Hypersaline Sediments in Western Australia. *Environ. Sci. Technol. 48:*9170-9178.

599 Ruecker, A., Weigold, P., Behrens, S., Jochmann, M., Barajas, X.L.O., Kappler, A. (2015)
600 Halogenated hydrocarbon formation in a moderately acidic salt lake in Western Australia –
601 role of abiotic and biotic processes. *Environ. Chem. 12*:406-414.

602 Schwertmann, U., Cornell, R.M. (2007) *The Iron Oxides, in: Iron Oxides in the Laboratory*. Wiley-
603 VCH Verlag GmbH, pp. 5–18.

604 Shen, Y., Buick, R., Canfield, D.E. (2001) Isotopic evidence for microbial sulphate reduction in
605 the early Archaean era. *Nature* 410:77–81.

606 Sorokin, D.Y., Tourova, T.P., Abbas, B., Suhacheva, M. V, Muyzer, G. (2012)
607 *Desulfonatronovibrio halophilus sp. nov.*, a novel moderately halophilic sulfate-reducing
608 bacterium from hypersaline chloride-sulfate lakes in Central Asia. *Extremophiles* 16:411–
609 417.

610

Squyres, S.W., Grotzinger, J.P., Arvidson, R.E., Bell, J.F., Calvin, W., Christensen, P.R., Clark, B.C., Crisp, J. A., Farrand, W.H., Herkenhoff, K.E., Johnson, J.R., Klingelhöfer, G., Knoll, A. H., McLennan, S.M., McSween, H.Y., Morris, R. V, Rice, J.W., Rieder, R., Soderblom, L. A. (2004) In situ evidence for an ancient aqueous environment at Meridiani Planum, Mars. *Science* 306:1709–1714.

Squyres, S.W., Arvidson, R.E., Bell, J.F., Calef, F., Clark, B.C., Cohen, B.A., Crumpler, L.A., De Souza, P.A., Farrand, W.H., Gellert, R. (2012) Ancient impact and aqueous processes at Endeavour Crater, Mars. *Science* 336:570–576.

Stern, J.C., Sutter, B., Freissinet, C., Navarro-González, R., McKay, C.P., Archer, P.D., Buch, A., Brunner, A.E., Coll, P., Eigenbrode, J.L., Fairen, A.G., Franz, H.B., Glavin, D.P., Kashyap, S., McAdam, A.C., Ming, D.W., Steele, A., Szopa, C., Wray, J.J., Martín-Torres, F.J., Zorzano, M.-P., Conrad, P.G., Mahaffy, P.R. the M.S.L.S. Team (2015) Evidence for indigenous nitrogen in sedimentary and aeolian deposits from the Curiosity rover investigations at Gale crater, Mars. *Proc. Natl. Acad. Sci. 112:*4245–4250.

Stevens, J.G., Khasanov, A.M., Miller, J.W., Pollak, H., Li, Z. (2002) *Mössbauer Mineral Handbook*. Mössbauer Effect Data Center.

Stoker, C.R., Zent, A., Catling, D.C., Douglas, S., Marshall, J.R., Archer, D., Clark, B., Kounaves, S.P., Lemmon, M.T., Quinn, R. (2010) Habitability of the Phoenix landing site. *J. Geophys. Res. Planets* 115.

Stookey, L.L. (1970) Ferrozine---a new spectrophotometric reagent for iron. *Anal. Chem.* 42:779–781.

Tehei, M., Zaccai, G. (2005) Adaptation to extreme environments: macromolecular dynamics in complex systems. *Biochim. Biophys. Acta (BBA)-General Subj.* 1724:404–410.

Timms, B. V. (2009) Study of the saline lakes of the Esperance Hinterland , Western Australia , with special reference to the roles of acidity and episodicity. *Natural Resources and Environmental Issues* 15, 44:215-225.

Timms, B. V. (2005) Salt lakes in Australia: Present problems and prognosis for the future. *Hydrobiologia* 552:1–15.

Tosca, N.J., Knoll, A.H., McLennan, S.M. (2008) Water activity and the challenge for life on early Mars. *Science* 320:1204–1207.

Van der Zee, C., Roberts, D.R., Rancourt, D.G., Slomp, C.P. (2003) Nanogoethite is the dominant reactive oxyhydroxide phase in lake and marine sediments. *Geology* 31:993-996.

Vargas, M., Kashefi, K., Blunt-Harris, E.L., Lovley, D.R. (1998) Microbiological evidence for Fe (III) reduction on early Earth. *Nature* 395:65–67.

Weigold, P., Ruecker, A., Loesekann-Behrens, T., Kappler, A., Behrens, S. (2015) Ribosomal tag pyrosequencing of DNA and RNA reveals “rare”taxa with high protein synthesis potential in the sediment of a hypersaline lake in Western Australia. *Geomicrobiol. J.*

Xiong, H., Liao, Y., Zhou, L. (2008) Influence of chloride and sulfate on formation of akaganeite and schwertmannite through ferrous biooxidation by acidithiobacillus ferrooxidans cells. *Environ. Sci. Technol. 42*:8681–8686.

653 Table 1. Geochemical characterization of Lake Orr and Lake Whurr sediments.

Sample	Leachable organic carbon [mg/L][a]	pH[b]	Water content [%][c]	Total Fe [%][d]	Total S [%][d]	Cl [%][d]	TOC [%][e]
Lake Orr 0-2 cm	1.7±0.1	3.8	11.4	0.2	n.d.	27.8	0.1±0.0
Lake Orr 2-8 cm	2.2±0.0	4.5	29.9	2.0	n.d.	4.5	0.4±0.0
Lake Orr >8 cm	9.6±0.2	4.8	46.4	2.4	n.d.	8.3	0.8±0.0
Lake Whurr orange	2.9±0.0	6.3	47.3	5.2	1.2	4.5	0.9±0.0
Lake Whurr red	6.7±0.0	5.4	39.9	16.2	0.7	3.3	1.8±0.1

654 [a]) Quantified in a sediment eluate by a High TOC Elementar Instrument (modified from
655 Emmerich *et al.* 2012). [b]) Measured in 0.01 M $CaCl_2$ after 2 hours. [c]) Dried at 105°C until weight
656 stability. [d]) [Weight % of dry sediment] quantified by XRF. N.d. = not determined in the samples
657 [e]) Weight % quantified by a C/N analyzer using a HCl-titrated sample (modified from Emmerich
658 *et al.* 2012). The range and standard deviation of duplicate (leachable organic carbon) and
659 triplicate (C_{org}) measurements are given.

660

Table 2. Quantification of Fe(II) and Fe(III) in Lake Whurr sediments using the spectrophotometric Ferrozine assay. Samples were either extracted with 1 M anoxic HCl for the “bioavailable”, poorly crystalline Fe-phase or with 6 M HCl for the “non-bioavailable”, crystalline Fe-phase.

Extraction	Sample	FeTotal µM	Fe(II) µM	Fe(III) µM	Fe(II)/Fe(III) %	Fe(II)/FeTotal %
1 M HCl	Orange	85.13	8.79	76.33	11.5	10.3
	Red	104.44	10.31	94.13	11.0	9.9
6 M HCl	Orange	42087.18	527.09	41560.09	1.3	1.3
	Red	45783.76	738.29	45045.47	1.6	1.6

670 Table 3. Mössbauer parameters for Lake Whurr. CS – center shift, ΔE_Q – mean quadrupole
671 splitting, B_{hf} – mean hyperfine fi*eld, Pop.* – relative abundance/population, *sp -
672 superparamagnetic.

673

Sample	Temp. K	Site	CS (mm/s)	ΔE_Q (mm/s)	B_{hf} (T)	Pop. %	Error ±
Lake Whurr Orange	295	Pyrite	0.36	0.54		11.5	0.5
		Jarosite	0.38	1.31		6.3	0.5
		Goethite	0.39	-0.25	19.2	45.2	0.7
		Hematite	0.38	-0.21	47.9	37.0	0.6
	77	Pyrite	0.45	0.51		8.9	1.6
		Jarosite	0.47	1.32		5.3	1.4
		Goethite	0.48	-0.21	48.6	41.6	5.7
		Hematite	0.48	-0.17	53.0	44.2	5.6
	5	Pyrite	0.46	0.55		9.0	0.7
		Jarosite	0.48	1.71		1.5	0.6
		Goethite	0.49	-0.21	50.4	50.3	2.7
		Hematite	0.49	-0.16	53.7	39.2	2.7
Lake Whurr Red	295	Pyrite + sp* hematite	0.36	0.62		13.6	0.4
		Poorly ordered Hematite	0.26	-0.14	37.4	19.4	1.6
		Hematite	0.38	- 0.21	47.1	67.0	1.3
	77	Pyrite + sp* hematite	0.45	0.69		15.0	0.2
		Hematite	0.51	-0.18	51.8	85.0	0.2
	5	Pyrite	0.46	0.55		13.5	0.2
		Jarosite	0.51	1.9		2.0	0.3
		Hematite	0.49	-0.17	53.1	84.5	0.4

674

675 Table 4. Fitting parameters of residual Lake Whurr sediment material left after digestion in 6 M
676 anoxic HCl at 70°C for 24 hours. CS – center shift, ΔE_Q – quadrupole splitting, σ – spread of
677 ΔE_Q, * indicates parameter was fixed during fitting.
678

Sample	**T K**	**CS mm/s**	**ΔE_Q mm/s**	**σ mm/s**
Orange	5	0.446	0.55*	1.40
Red	5	0.458	0.55*	1.54

679
680

Table 5. Mössbauer parameters for Lake Orr. CS – center shift, ΔE_Q – mean quadrupole splitting, B_{hf} – mean hyperfine field, Pop. – relative abundance/population.

Sample	Temp. K	Site	CS (mm/s)	ΔE_Q (mm/s)	B_{hf} (T)	Pop. %	Error ±
2-5 cm	295	Fe(III)	0.36	0.97		97.4	1.3
		Fe(II)	1.29	2.29		2.6	1.3
	77	Fe(III)	0.46	0.96		83.1	2.7
		Fe(II)	1.22	3.05		3.4	1.8
		Goethite	0.48	-0.24	49.6	13.6	2.4
	5	Fe(III)	0.45	0.95		66.9	4.5
		Fe(II)	1.38	2.52		5.6	4.5
		Goethite	0.46	-0.29	49.4	27.5	3.6
5-8 cm	295	Fe(III)	0.35	0.93		81.9	2.2
		Fe(II)	1.29	2.22		5.3	1.6
		Goethite	0.38	0.00	30.1	12.8	1.8
	77	Fe(III)	0.47	0.98		97.3	1.8
		Fe(II)	1.16	3.03		2.7	1.8
	5	Fe(III)	0.48	1.39		76.5	2.0
		Fe(II)	1.30	2.50		2.0	0.9
		Goethite	0.33	-0.25	48.0	21.5	1.9

FIGURE LEGENDS

FIG. 1. Location of the field site in Australia **(A),** sediment characteristics of Lake Whurr 2013 **(B)** and Lake Orr 2012 **(C),** and differences in the appearance of Lake Whurr after rain events in the Australian autumn of 2013 **(D)** and desiccated bed of Lake Orr in autumn 2012 **(E)**.

FIG. 2. Concentrations of different Fe fractions in a sediment profile of Lake Orr in µg/g dry sediment. **(A)** 0.5 M HCl extractable ("poorly crystalline" Fe). **(B)** 6 M HCl extractable ("crystalline" Fe). Error bars give standard deviations from duplicate measurements. B.d.l. means below detection limit.

FIG. 3. X-ray diffraction pattern of red and orange samples from Lake Whurr sediments. The bottom panel shows reference diffraction patterns of goethite, hematite and halite and a diffraction pattern of the Si-wafer.

FIG. 4. ^{57}Fe Mössbauer spectroscopy of **(A)** orange and **(B)** red samples of Lake Whurr sediments at temperatures of 275 K, 77K and 5K. * indicates the tentative identification of pyrite and jarosite, a.u. = arbitrary units

FIG. 5. ^{57}Fe Mössbauer spectroscopy of **(A)** orange and **(B)** red samples of Lake Whurr at 5 K after digestion in 6 M anoxic HCl at 70°C for 24 hours. Shown are the raw data (gray) and the sum of fits (orange/red), a.u. = arbitrary units.

FIG. 6. ^{57}Fe Mössbauer spectroscopy of samples from **(A)** 2-5 cm and **(B)** 5-8 cm depth of Lake Orr sediments at temperatures of 275 K, 77 K and 5 K, a.u. = arbitrary units.

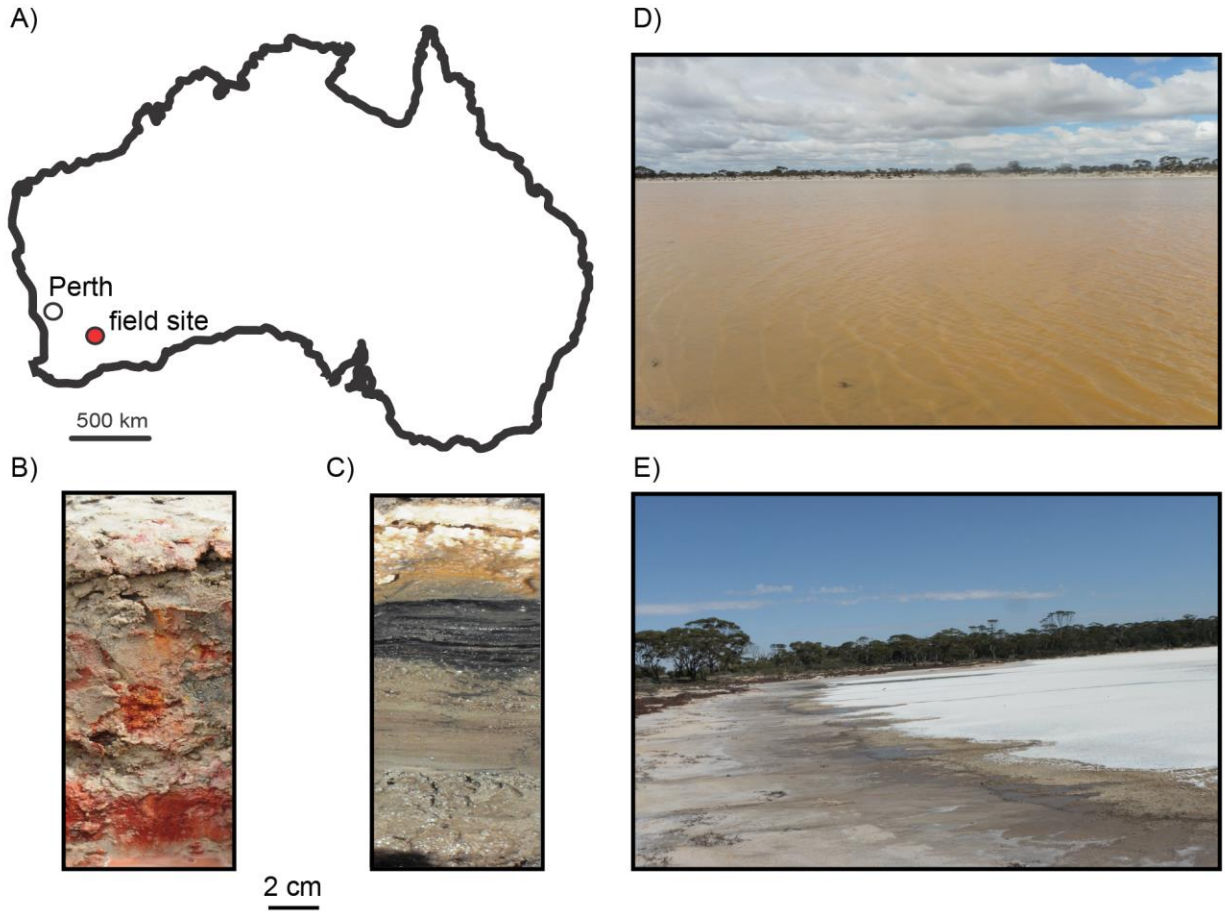

712

713

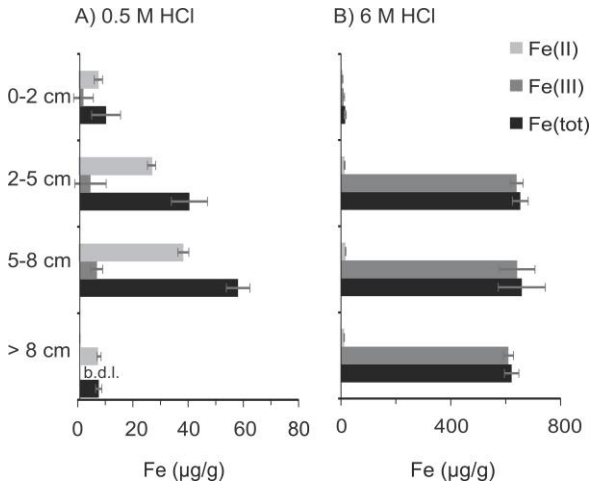
A) 0.5 M HCl
B) 6 M HCl
Fe(II)
Fe(III)
Fe(tot)
0-2 cm
2-5 cm
5-8 cm
> 8 cm
b.d.l.
0
20
40
60
80
0
400
800
Fe (µg/g)
Fe (µg/g)

714

715

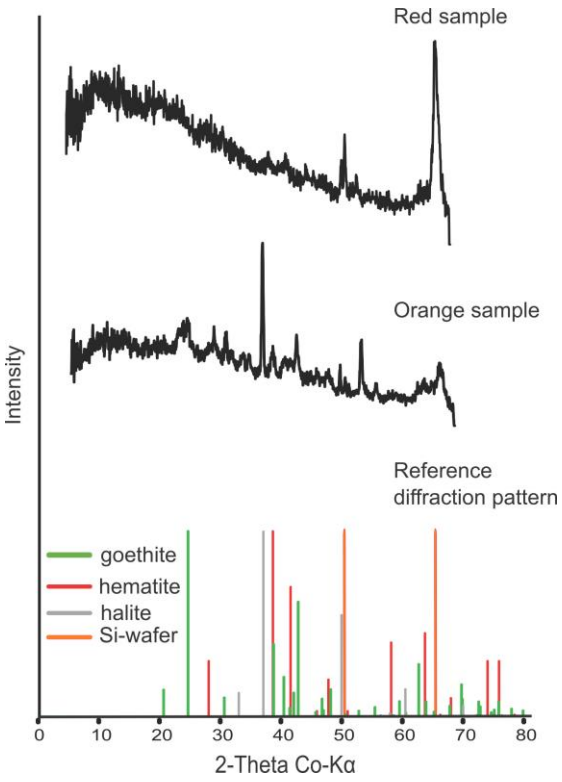
Red sample
Orange sample
Intensity
Reference
diffraction pattern
goethite
hematite
halite
Si-wafer
0
10
20
30
40
50
60
70
80
2-Theta Co-Kα

716

717

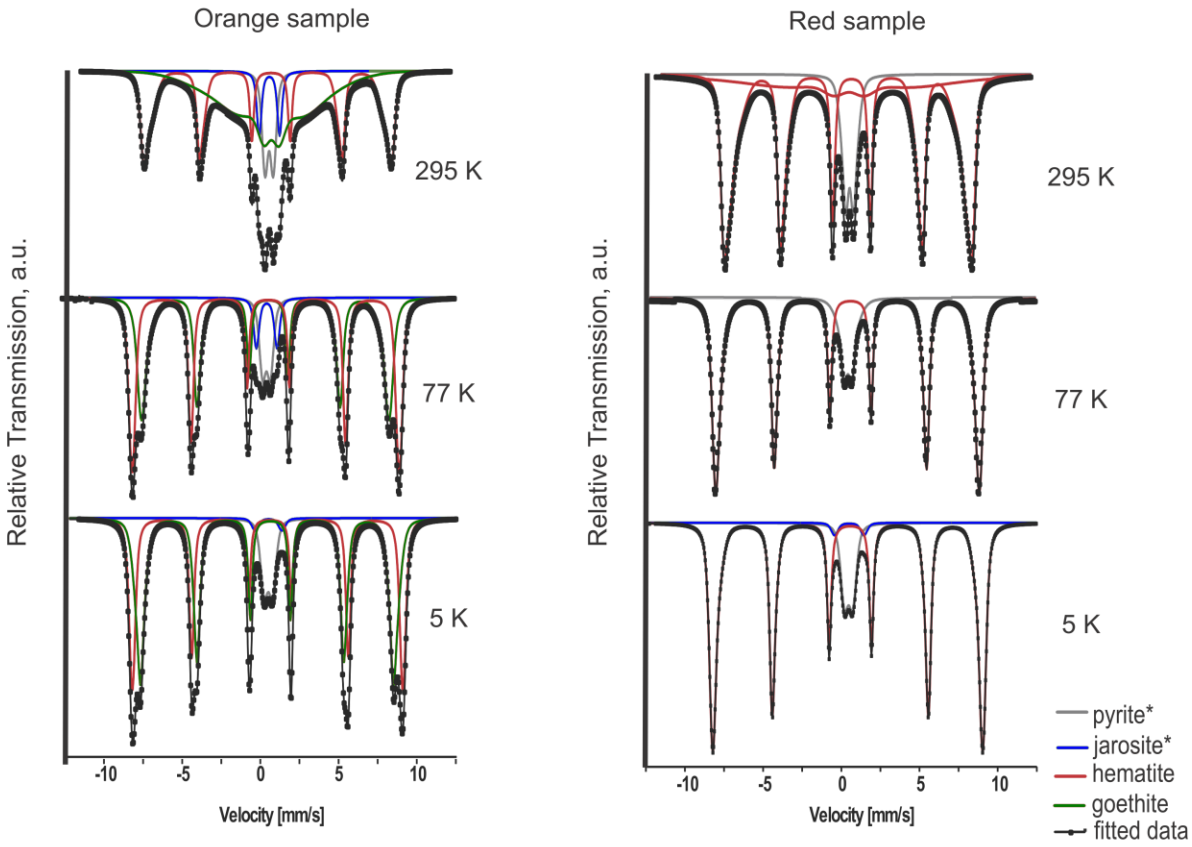
Orange sample
Red sample
Relative Transmission, a.u.
295 K
77 K
5 K
-10
-5
0
5
10
Velocity [mm/s]
pyrite*
jarosite*
hematite
goethite
fitted data

718

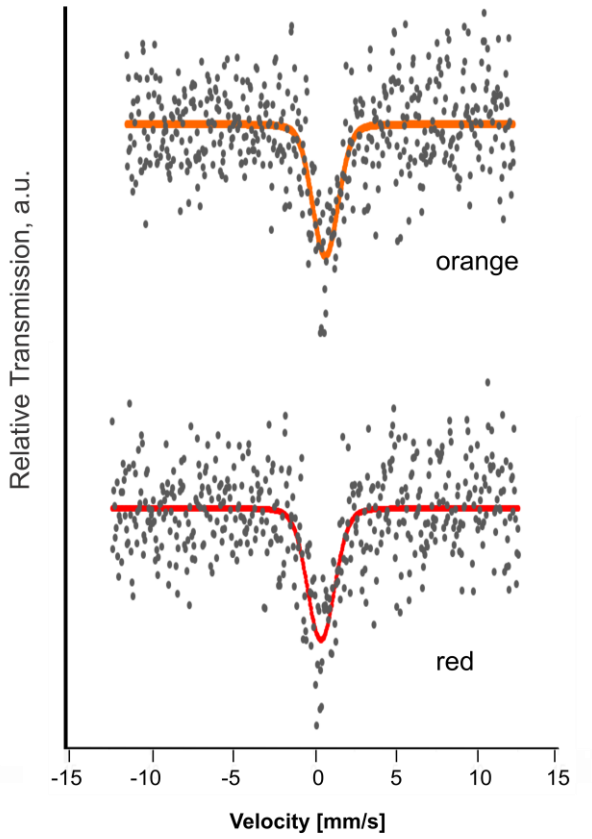
Relative Transmission, a.u.
orange
red
-15
-10
-5
0
5
10
15
Velocity [mm/s]

719

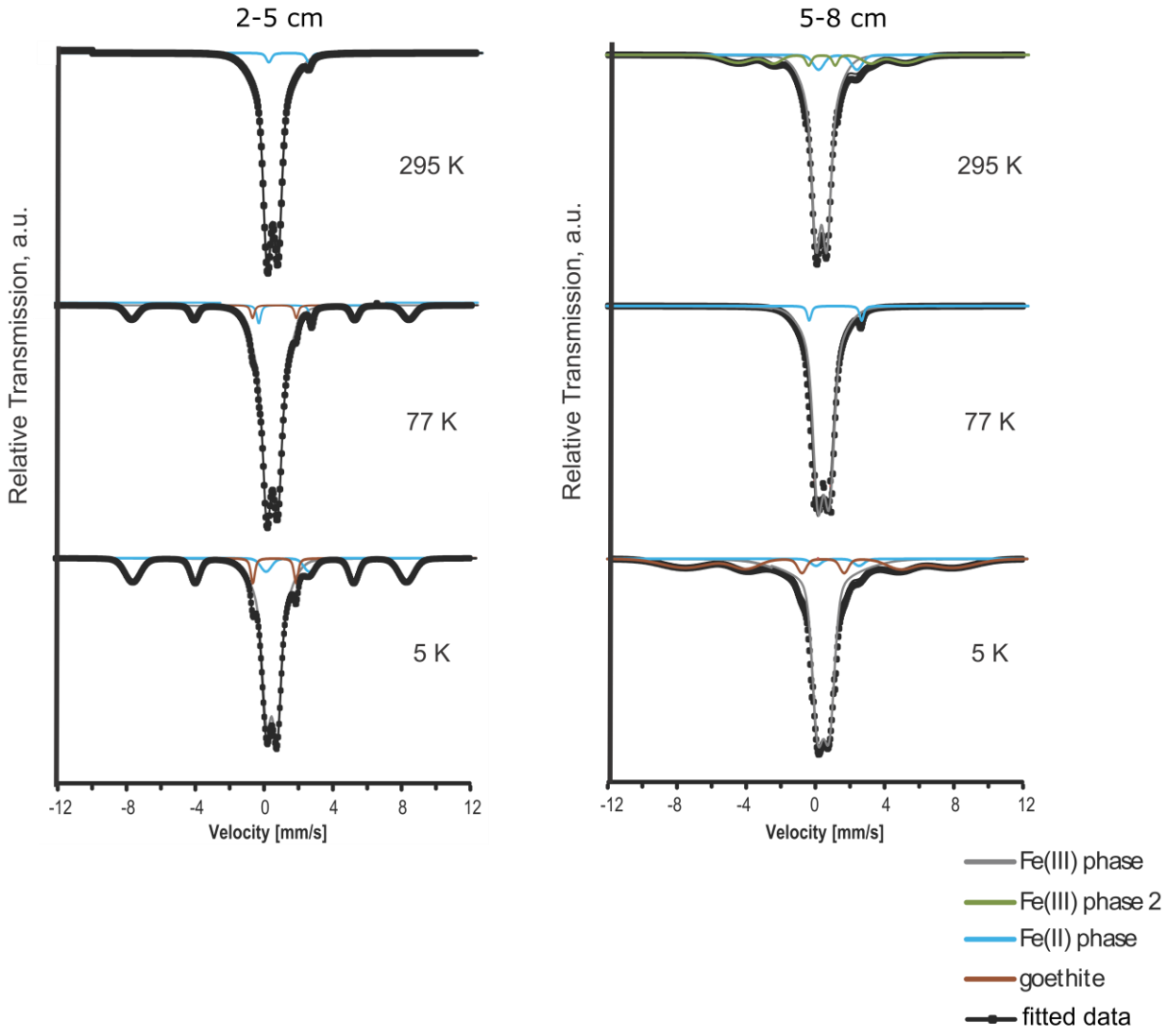

720

721

722

723

724

725